Supporting Information

Clark-Hachtel et al. 10.1073/pnas.1304332110

Materials and Methods

Beetle Cultures. The beetle cultures were reared on whole wheat flour [+5% (wt/wt) yeast] at 30 °C in a temperature and humidity controlled incubator. An enhancer trap line *pu11*, which has enhanced yellow fluorescent protein (EYFP) expression in the hindwing and elytron discs (Fig. S4) (1, 2), was used for all RNAi experiments. Cx^{6} and Cx^{apt} were used as *Scr* loss-of-function mutants (3–5). Cx^{apt}; *pu11*; *p* beetles were crossed with Cx^{6}/*Es* beetles to obtain Cx^{apt}/Cx^{6}; *pu11*; *p* beetles.

Fly Strains. The genotypes of flies used in this work were as follows: w^{1118}; P{GD1558}v16896 (*vg* RNAi), y^{1} w^{1118}; P{w[+mW.hs]=GawB}tsh^{md621}/CyO; P{w[+mC]=UAS-y.C}MC1/TM2 (*tsh* Gal4), P{w[+mC]=UAS-Dcr-2.D}1, w^{1118}; P{w[+mC]=Act5C- GAL4}25FO1/CyO (Act5C Gal4), y^{1} w^{1118}; P{w[+mC]=vgMQ-GAL4.Exel}3 (*vg* Gal4). *vg* RNAi line was obtained from Vienna Drosophila RNAi Center, and three Gal4 lines were obtained from Bloomington Stock Center.

Gene Cloning and dsRNA Synthesis. The *Tribolium* ortholog of *Drosophila dsh* was identified via BLAST analysis. *Tribolium* pupal cDNA was used to clone the cDNA fragment into PCR4-TOPO vector (PCR4-TOPO-TA cloning kit; Invitrogen). The primers used to clone the *dsh* fragment are provided in Table S1. Detailed cloning of two *apterous* (*ap*) genes, *vestigial* (*vg*) and *nubbin* (*nub*) from *Tribolium*, has been described (6). The dsRNA templates were synthesized by PCR using the TOPO_RNAi primer (7, 8), or gene specific primers with the T7 polymerase promoter sequence at the 5′ end. dsRNAs were synthesized by in vitro transcription (Megascript T7; Ambion) using 1.5 μg of templates. The resulting dsRNA samples were then purified by Megaclear kit (Ambion). Specificity of the products was confirmed via agarose gel electrophoresis. Concentration of dsRNA ranged from 5 to 7 μg/uL. The sequence and primers used to clone *dsh* are available in GenBank (see Table S1 for the accession number).

***Tribolium* Injection.** Injections were performed in the last larval stage or penultimate larval stage. EYFP expression in *pu11* developing wing and elytron discs was used to select appropriate larval stages. Stereo microscopes (Zeiss Stemi 2000 and Discovery v12) were used for the injections. At least 20 larvae were used for each set of injections. Approximately 0.7–0.9 μL of 1 μg/μL dsRNA solution was injected into each larva. After injection, the larvae were kept in flour at 30 °C until they became adults for phenotypic analysis. The detailed injection protocol can be found in ref. 7.

Off-Target Effect Assessment. The absence of off-target effect was confirmed when RNAi for the two nonoverlapping regions of *vg* produced the same phenotypes, which were the same as the phenotypes produced by the longer fragment RNAi. The detailed primer information for these nonoverlapping fragments can be seen in Table S1. The corresponding locations of these fragments relative to the longer fragment are also provided in Table S1.

Inverse PCR and RACE. Inverse PCR was performed by using the protocol established by Berkeley *Drosophila* Genome Project (9) with some modifications. The primer sequences are provided in the Table S1. Three restriction enzyme sites (Sau3A I, Csp6, and Hha I) were used. Genomic DNA was isolated from five *pu11* pupae by using DNeasy Blood & Tissue Kit (Qiagen) and then digested by the restriction enzymes. After self-ligation at 4 °C overnight, inverse PCR was performed with the primer sets in Table S1. RACE was performed by using GeneRacer Advanced RACE Kit (Invitrogen) with total RNA isolated from *pu11* pupae. The sequences of the *pu11* insertion site and the two isoforms of *nub* cDNA have been submitted to GenBank.

In Situ Hybridization. In situ hybridization was performed by using a protocol previously published as a supplemental document in Tomoyasu et al. (6). The DNA template for *nub* riboprobe was made via PCR (see Table S1 for the primer sequences).

Image Processing and Documentation. The *Tribolium* whole body and wing tissues were fixed in 95% ethanol at least overnight. Wing tissues were then dissected and mounted on microscopic glass slides by using Permount. The images were captured by using Zeiss AxioCam MRc5 with AxioPlan 2 (dissected tissues and embryos) or Zeiss Discovery V12 (whole adults). Zeiss AxioVison Extended Focus module was used to obtain images with increased focus depth. Some pictures were enhanced only for brightness and contrast with Adobe Photoshop.

1. Lorenzen MD, et al. (2003) piggyBac-mediated germline transformation in the beetle Tribolium castaneum. *Insect Mol Biol* 12(5):433–440.
2. Tomoyasu Y, Wheeler SR, Denell RE (2005) Ultrabithorax is required for membranous wing identity in the beetle Tribolium castaneum. *Nature* 433(7026):643–647.
3. Beeman RW, Stuart JJ, Haas MS, Denell RE (1989) Genetic analysis of the homeotic gene complex (HOM-C) in the beetle Tribolium castaneum. *Dev Biol* 133(1):196–209.
4. Curtis CD, et al. (2001) Molecular characterization of Cephalothorax, the Tribolium ortholog of Sex combs reduced. *Genesis* 30(1):12–20.
5. Shippy TD, Rogers CD, Beeman RW, Brown SJ, Denell RE (2006) The Tribolium castaneum ortholog of Sex combs reduced controls dorsal ridge development. *Genetics* 174(1):297–307.
6. Tomoyasu Y, Arakane Y, Kramer KJ, Denell RE (2009) Repeated co-options of exoskeleton formation during wing-to-elytron evolution in beetles. *Curr Biol* 19(24): 2057–2065.
7. Philip BN, Tomoyasu Y (2011) Gene knockdown analysis by double-stranded RNA injection. *Methods Mol Biol* 772:471–497.
8. Tomoyasu Y, et al. (2008) Exploring systemic RNA interference in insects: a genome-wide survey for RNAi genes in Tribolium. *Genome Biol* 9(1):R10.
9. Rehm EJ, Berkeley Drosophila Genome Project (2002) Inverse PCR & cycle sequencing of P element insertions for STS generation. Available at http://www.fruitfly.org/about/methods/inverse.pcr.html. Accessed July 3, 2002.

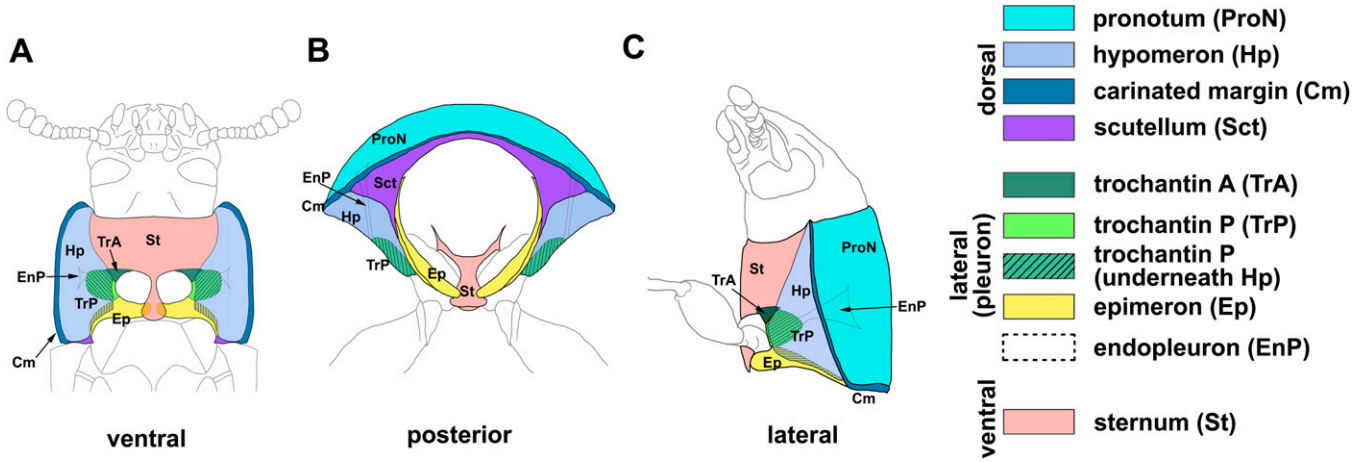

Fig. S1. *Tribolium* body wall annotation. A detailed annotation of *Tribolium* T1 body wall structures is shown. Ventral (*A*), posterior (*B*), and lateral (*C*) view. The annotation is based on El-Kifl (1), except hypomeron has been included based on Hlavac (2). The internal sclerotized tendon identified in El-Kifl 1953 was also reannotated as endopleuron based on Hlavac (2).

1. El-Kifl (1953) Morphology of the adult Tribolium confusum Duv. and its differentiation from Tribolium (Stene) castaneum Herbst. *Bulletin de la Société Fouad Ier d'Entomologie* 37:173–249.
2. Hlavac TF (1972) The prothorax of Coleoptera: Origin, major features of variation. *Psyche* 79(3):123–149.

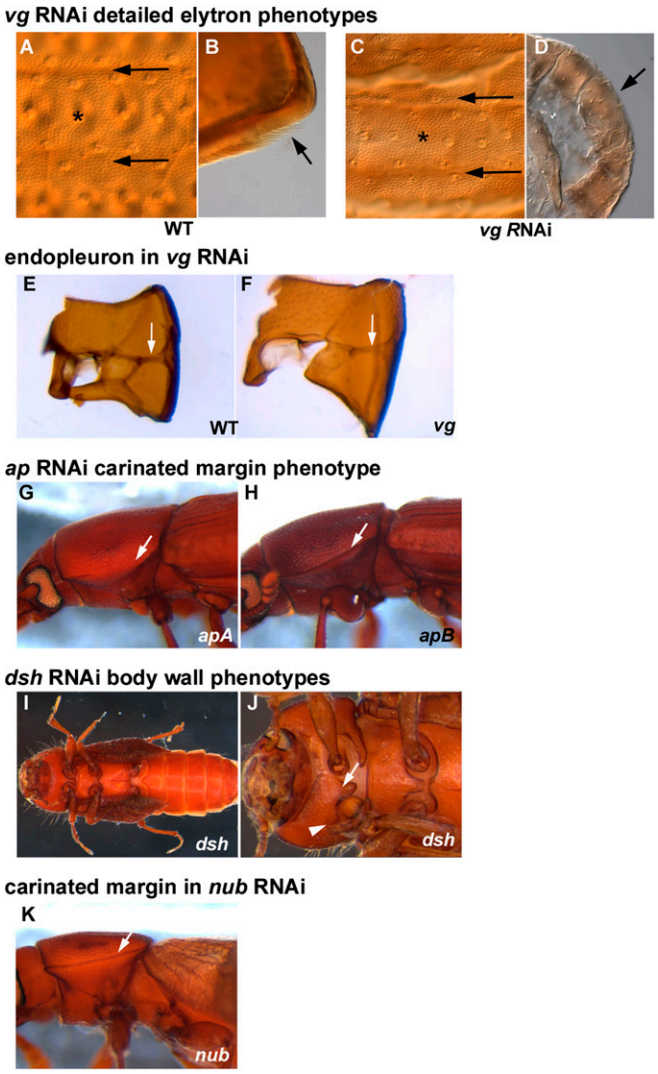

Fig. S2. RNAi phenotypes of wing genes. (*A–D*) Reduction in elytron size is a result of margin structure deletion. (*A* and *B*) Wild-type and (*C* and *D*) *vg* RNAi elytron. Vein and sensory structures in eytron (arrows and asterisk in *A* and *C*) are intact, while margins are truncated (arrows in *B* and *D*). (*E* and *F*) Internal view of T1 showing endopleuron. (*E*) Wild type. (*F*) *vg* RNAi T1. The endoplueron (white arrow in *E* and *F*) is unaffected by *vg* RNAi. (*G* and *H*) *ap* RNAi carinated margin phenotypes. (*G*) *ap*A RNAi. (*H*) *apB* RNAi. The carinated margin is missing in *apA* but not in *apB* (arrows in *G* and *H*). (*I* and *J*) *dsh* RNAi. The distal leg is atrophied (*I*), and the sternum is drastically reduced (arrow in *J*). The pleural plates appear to be less affected (arrowhead in *J*). (*K*) *nub* RNAi. The carinated margin is unaffected (arrow).

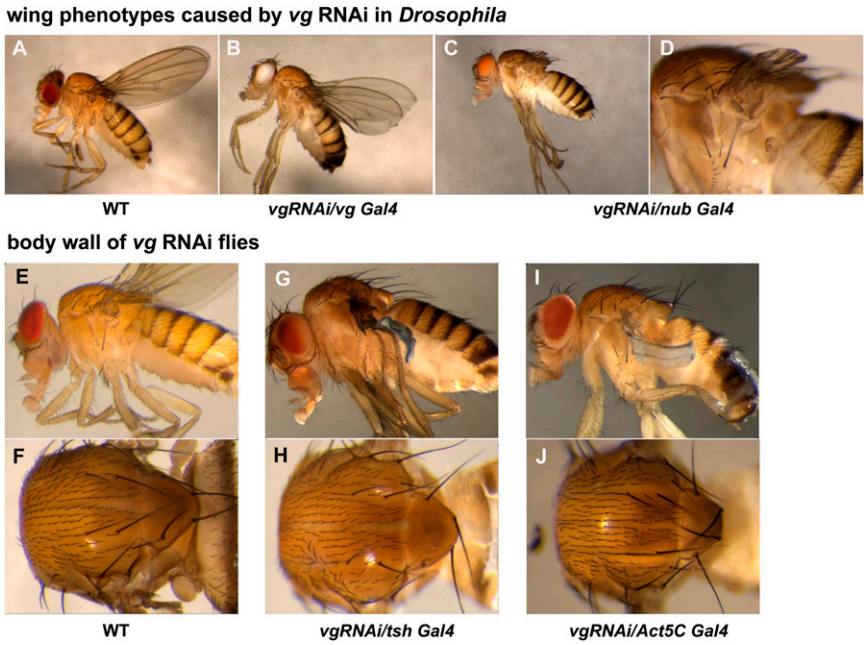

Fig. S3. *vg* RNAi phenotypes in *Drosophila*. (*A–D*) *vg* is essential for proper wing formation in *Drosophila*. (*A*) Wild type. (*B*) *vg* Gal4 > *vg* RNAi. The margin of the wing is affected (arrow). (*C*) *nub* Gal4 > *vg* RNAi. (*D*) Closeup of *C*. Wing is severely reduced. These results are consistent with previous studies with *vg* mutants, indicating that the *vg* RNAi is working properly. (*E–J*) Body wall of *vg* RNAi in *Drosophila* (*E, G,* and *I*). Lateral view of adult flies. (*F, H,* and *J*) Dorsal view of adult notum. (*E* and *F*) Wild type. (*G* and *H*) *tsh* Gal4 > *vg* RNAi. (*I* and *J*) *Act5C* Gal4 > *vg* RNAi. No noticeable body wall disruption was observed, indicating that *vg* is dispensable for proper body wall development in *Drosophila*.

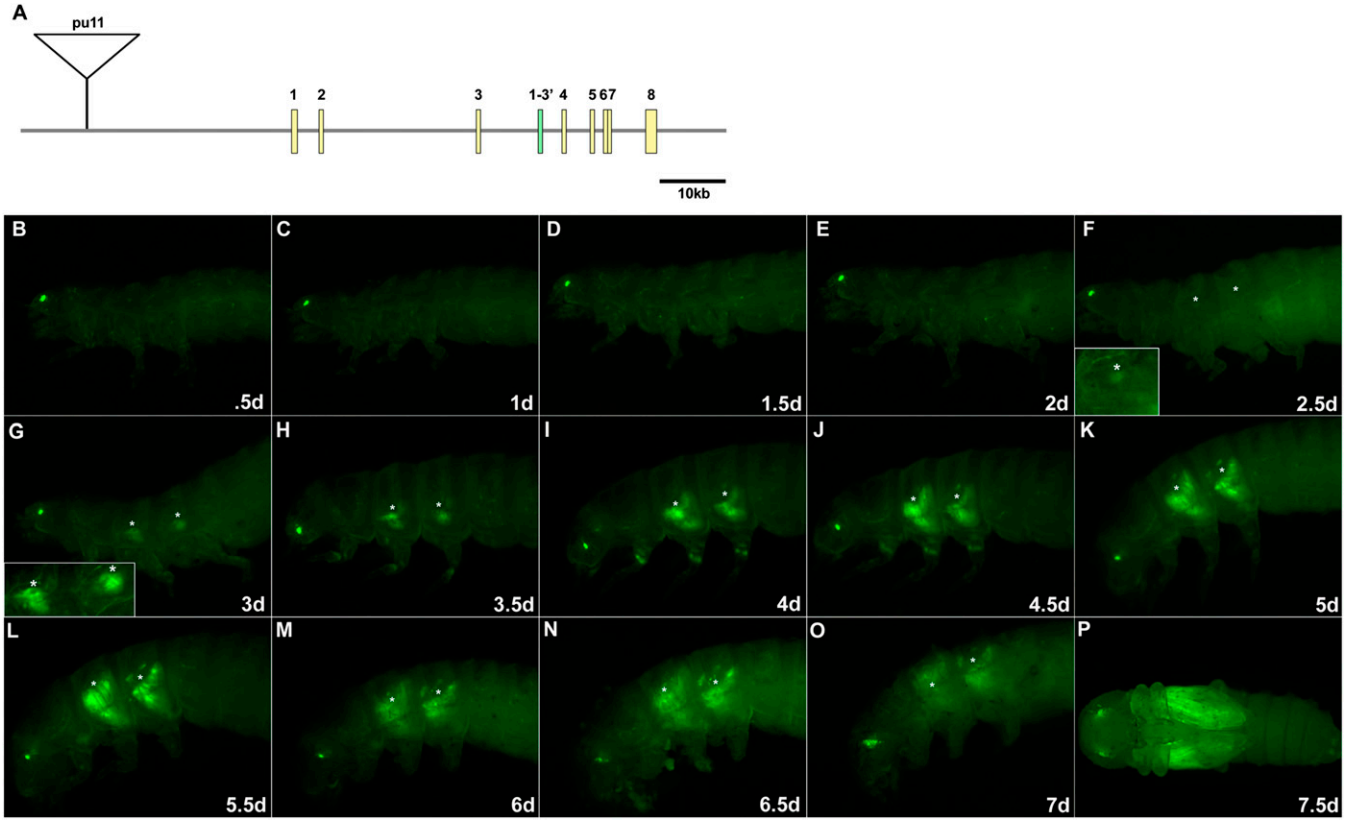

Fig. S4. *pu11* is a *nub* enhancer trap line. (*A*) *nub* gene structure and the *pu11* insertion site. The numbered boxes indicate *nub* exons. The green exon (1-3′) is an alternative first exon. (*B–O*) *pu11* larval development during the last larval stage (days after the last larval molt are indicated). Wing and elytron discs begin to express EYFP at 2.5 d (white asterisks in *F*) and continue to express EYFP in these discs throughout the rest of the last larval stage (white asterisks in *G–O*). (*P*) Pupal stage. Inverse PCR revealed that *pu11* carries a single insertion upstream of *nub*. RACE analysis along with exon/intron identification by Splign (National Center for Biotechnology Information) have revealed that the *pu11* insertion is ∼30 kb upstream of the *nub* coding region (*A*). The EYFP expression pattern in the elytron and hindwing discs are consistent with the in situ hybridization pattern of *nub* (Tomoyasu et al.; ref. 1), indicating that *pu11* traps the *nub* wing enhancer. *pu11* also displays unique neuronal expression that is not visible in other 3xP3 transgenic beetles (see Fig. 4 for the neural expression), suggesting that *pu11* also traps the *nub* neuronal enhancer. We analyzed the detailed expression pattern of *pu11*/*nub* enhancer activity during the last larval stage by monitoring the EYFP expression every 12 h (*B–O*). Initially, two pairs of small clusters of cells, each located in T2 and T3, respectively, start expressing EYFP about 50 h after the last larval molt (asterisks in *F*). These clusters grow rapidly to form mature elytron and hindwing discs at the end of the last larval stage (*O*).

1. Tomoyasu Y, Arakane Y, Kramer KJ, Denell RE (2009) Repeated co-options of exoskeleton formation during wing-to-elytron evolution in beetles. *Curr Biol* 19(24):2057–2065.

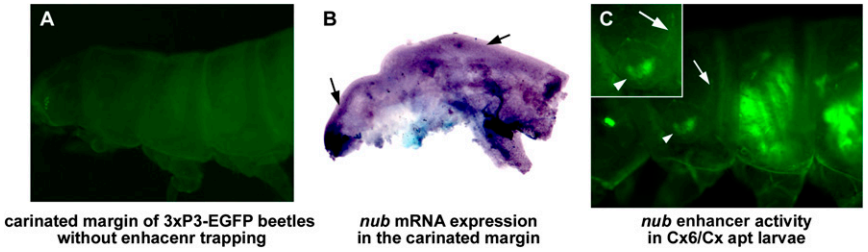

Fig. S5. *nub* activity in the developing carinated margin. (*A*) EGFP expression is absent from a 3xP3 transgenic line without enhancer trapping, indicating that the carinated margin expression is unique to the *nub* enhancer trap line. (*B*) *nub* mRNA expression in the larval carinated margin. In situ hybridization for *nub* detected a weak signal along the future carinated margin (arrows). Anterior is to the left. (*C*) *nub* enhancer activity in the Cx^{6}/Cx^{apt} larvae. Carinated margin expression is absent when carinated margin outgrowth is present (arrowheads) although neuronal expression persists (arrows). *C Inset* is the magnified image of T1.

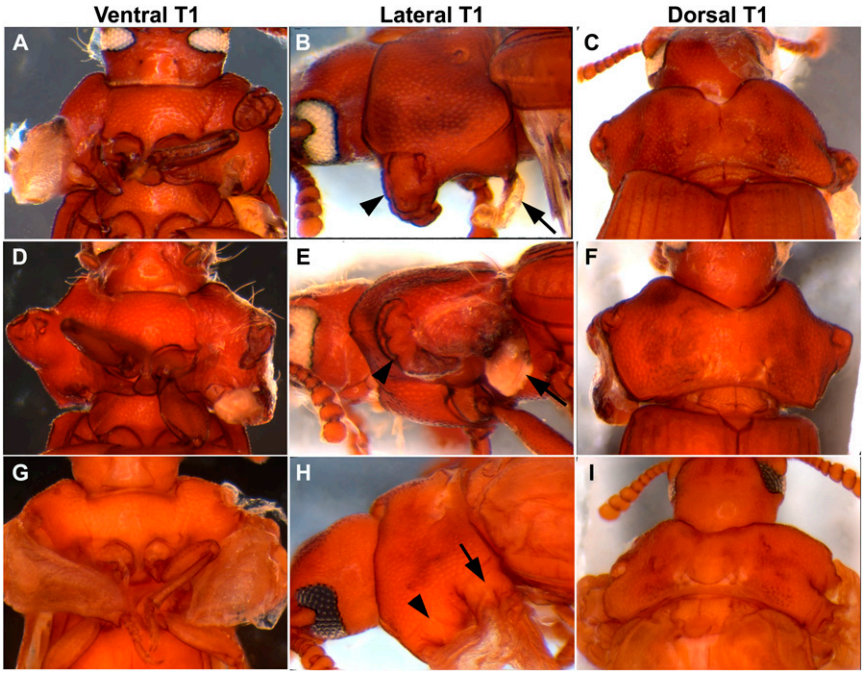

Fig. S6. Cx^{6}/Cx^{apt} intermediate phenotypes. Various degrees of transformation observed in Cx^{6}/Cx^{apt} beetles. Ventral, lateral, and dorsal views of three representative individuals are shown (*A–C*, *D–F*, and *G–I*). The carinated margin outgrowth and the pleural outgrowth are indicated by arrowhead and arrow in *B, E*, and *H*, respectively. The formation of the ectopic elytron is incomplete when the two outgrowths remain separated (*B* and *E*). Merger of the two outgrowths produces a more complete elytron (*H*).

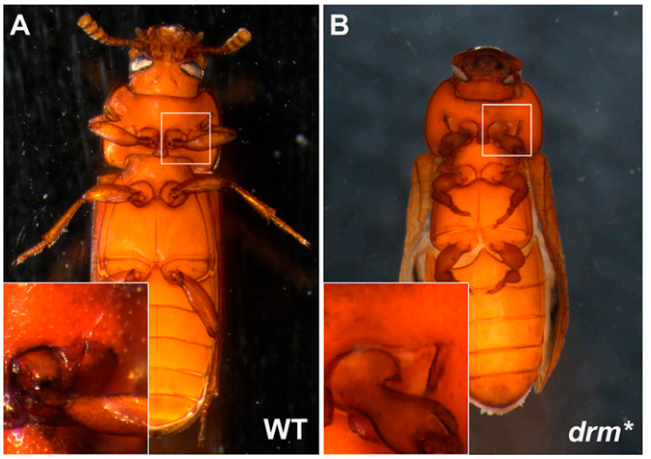

Fig. S7. *odd-skipped* family genes are required for proper pleural plate formation in *Tribolium*. (*A*) Wild type. (*B*) *drm* RNAi (which targets the entire *odd-skipped* family). The trochantin is greatly reduced (*Inset*). The *odd-skipped* family of genes is composed of four paralogs: *odd-skipped* (*odd*), *sister of odd and bowl* (*sob*), *brother of odd with entrails limited* (*bowl*), and *drumstick* (*drm*), each of which codes for an evolutionarily conserved Zinc finger transcription factor. Surprisingly, the nucleotide sequences that code for the Zinc finger domain are highly similar among the paralogs, thus allowing us to target the entire family simultaneously with a single RNAi knockdown. *drm*, the shortest of these four paralogs, is composed almost entirely of this sequence. We constructed dsRNA (216 bp) that covers this region (Table S1). In addition to leg segmentation defects (which may reflect the evolutionarily conserved function of this family), *drm* RNAi resulted in a reduction of pleural structures in the T1 segment (*B*).

Table S1. cDNA and genomic fragments used in this study

Sequence name	GenBank accession no.	Fragment name	Length, bp	Primer 1 sequence	Primer 2 sequence	Notes
vg partial cds	FJ647800	vg F1R3	856	tccttacttgtacca aagggccg	ctcttcttatcctactatg tcaggtgtg	—
vg nonoverlap fragment 1	N/A	VGi F1R1	315	cgtttggggccgc acatcagtat	gacgatgattcccaagacg ccg	Fragment used to exclude OTE. Corresponds to nt 81–395 of vg F1R3
vg nonoverlap fragment 2	N/A	VGi F2R2	317	gccggaagttca cgtgctcaatac	cttttacttccgggatcca ggctg	Fragment used to exclude OTE. Corresponds to nt 447–823 of vg F1R3
dishevelled (dsh) partial cds	KC688264	dsh F1R1	515	gtcgcccttga tggtagaatagaa	gtcgcgacgctcctgaaa	
drumstick (drm)	KF684967	drm F1R1	216	gttagtgggcgcga gttccgtaga	ttaccgccatatgcattga ttaca	
nub riboprobe template	N/A	nub F5R5	685	ttacaaaaccaggt ccaacaaatc	agaaccacacgcgcacca cctc	The reverse side was amplified with T7 on the cloning vector
nub full-length cds long isoform	KC688265	—	2,919	N/A	N/A	Longer isoform that contains exon 1, 2, and 3. See Fig. S3
nub full-length cds short isoform	KC688266	—	2,264	N/A	N/A	Shorter isoform that contains an alternative first exon (exon1-3′). See Fig. S3
pu11 insertion site	KC688267	—	765	N/A	N/A	Genomic sequence near the pu11 insertion site.

N/A, not applicable.